Civil Engineering Infrastructures Journal, 53(2): 295 – 311, December 2020
Print ISSN: 2322-2093; Online ISSN: 2423-6691
DOI: 10.22059/ceij.2019.284169.1594

Research Paper

Estimation of Damping for a Double-Layer Grid Using Input-Output and Output-Only Modal Identification Techniques

Salehi, S.[1], Davoodi, M.R.[2*] and Mostafavian, S.A.[3]

[1] Ph.D. Candidate, Structural Engineering, Faculty of Civil Engineering, Babol Noshirvani University of Technology, Babol, Iran.
[2] Associate Professor, Faculty of Civil Engineering, Babol Noshirvani University of Technology, Babol, Iran.
[3] Assistant Professor, Department of Civil Engineering, Payame Noor University (PNU), Tehran, Iran.

Received: 24 Jun. 2019; Revised: 24 Sep. 2019; Accepted: 30 Sep. 2019

ABSTRACT: In large civil engineering structures, the output-only modal identification is the most applicable technique for estimating the modal parameters such as damping. However, due to no measurement and control of excitation force, the identified parameters obtained by output-only technique have more uncertainty than those derived from the input-output technique. Given the different nature and uncertainties of the two modal identification techniques, in the present study, the damping related to the first 12 modes of a double-layer grid developed from the ball joint system were identified via the two techniques and compared with each other. For this purpose, a double-layer grid was constructed by pipes and balls with free-free boundary conditions provided for both input-output and output-only experiments. Exciting the grid, its acceleration response was measured at appropriate degrees of freedom. Then, by using these data and performing modal analysis, involving four different methods of input-output and five different methods of output-only, the natural frequencies and damping ratios of the desired modes were extracted. The results indicated that despite the good agreement between the modal damping of the grid, as identified by different methods of input-output together and by different methods of output-only together, the results of input-output and output-only methods were different with each other. The damping values through the input-output modal identification methods were on average 65% higher than the corresponding values of the output-only modal identification methods.

Keywords: Damping, Double-Layer Grid, Input-Output Techniques, Modal Testing, Output-Only Techniques.

INTRODUCTION

Structural identification has been applied in various fields such as Structural Health Monitoring (SHM), Finite Element model updating and damage detection (Rezaifar and Doost Mohammadi, 2016; Yasi and Mohammadizadeh, 2018). The SHM system is classified into broad categories namely: i) On-line SHM; ii) Off-line SHM and; iii)

* Corresponding author E-mail: davoodi@nit.ac.ir

Hybrid SHM system (Qarib and Adeli, 2015). At on-line SHM system; the necessary measurement system to acquire and store the sensors data would also be part of the on-board instrumentation An off-line SHM system does not necessitate any of the SHM system components to become part of the structure (Perez-Ramirez et al., 2019; Dertimanis et al., 2019). Non-Destructive Evaluation technologies for structural inspection is one of the best example for this category. In hybrid SHM system, there could be a combination of these components wherein some of them could be either on-board or off-line (Sony et al., 2019; Cardoso et al., 2019). Further information about on-line and hybrid SHM systems are presented in Azam et al. (2017) and Qarib and Adeli (2016). This work was focused on the off-line SHM and the identification of damping ratios of a structure.

The complexity of the damping phenomenon is due to multiplicity of terms to describe the loss of energy in a structure. Meanwhile, there are no analytical methods for evaluating all mechanisms of damping in real structures (Phani and Woodhouse, 2007). Consequently, experimental methods are adopted to estimate the damping ratio in structures. The most common method for a practical experiment of vibration is the modal testing. The effect of all different damping mechanisms is considered via a modal damping ratio for each vibration mode in modal analysis (Chopra, 2001).

The experimental determination of modal damping ratios as a structural parameter occurs via two identification techniques: input-output and output-only (Davoodi et al., 2017). In the former, damping ratios are determined based on the information received simultaneously through input (excitation) and output (response), while in the latter, damping ratios are determined based on the information acquired only from structure’s output. The input-output modal identification technique is mainly applicable for laboratory environment and small controllable structures (Davoodi et al., 2012a), while in real and large structures, modal parameters such as damping are primarily driven by the output-only modal technique (Brincker and Kirkegaard, 2010; Brincker et al., 2003). Due to the different nature of the test and uncertainties in the two mentioned techniques, comparison of damping results is indispensable.

There are some limited reports on damping comparison of both input-output and output-only techniques. Giraldo et al. (2009) compared the modal parameters of a structure using the input-output and output-only approaches. Their result indicated a great discrepancy between damping ratios obtained from the two techniques. Beskhiran et al. (2013) determined the modal parameters of a 13-story concrete block building located in Auckland University using the input-output and output-only modal identification techniques. Their results revealed that despite the good agreement between the obtained damping through different output-only methods, these values differed from damping results acquired through input-output methods. Gomes et al. (2018) obtained the modal parameters of Baixo Sabor Dam using both input-output and out-put-only identification methods. They found that the values obtained for damping in output-only methods were slightly lower in the case of input-output analysis. Sestieri and D'Ambrogio (2003) compared the identified parameters of a plate between input-output and output-only data. They observed that the damping ratios determined from input-output approach were almost double that of output-only one. Avitable (2006) compared the damping ratios obtained from the input-output and output-only methods for a ski-board and demonstrated that the output-only modal identification methods always provide a higher estimate of actual damping values, especially in Linear Time Invarient (LTI) systems. This conclusion has also been presented in Lauwagie et al. (2006). Mbarek et al. (2018) compared the modal parameters of a gearbox with the input-output and output-only methods and concluded that the difference between the identified damping values was considerable in both methods. Their results suggested that the output-only identification method was not able to identify all modes of the structure due to the stationary conditions of the signals and detected fewer modes compared to input-output method. Thibault et al. (2012) compared input-output and output-only modal identification methods for some case studies of structures, ranging from simple geometry to very complex ones. They observed that the damping results obtained from the two methods are different. They concluded that the deviation of damping ratios identified between the two methods was smaller for structures with a simple geometry and greater for structures with a complex geometry. Orlowitz and Brandt (2017) showed that for a structure with a simple behavior, such as a simple plate, the validation of damping estimates from output-only method is similar to estimates from input-output method. They reasoned that the cause of the difference between the results of damping detected by the two methods of input-output and output-only is due to different structural support conditions in both tests. They acquired modal damping for a plate using the methods of input-output and output-only with completely identical conditions in both experiments. They observed that there is no significant difference in the damping ratios identified by the two methods.

According to the above-mentioned reports, the researchers did not reach a consensus in the case of differences in the results of the two methods. In the current paper, the subject of damping identification was evaluated using the techniques of input-output and output-only modal analysis for a double-layer grid with a complex behavior due to a large number of elements and joints (Davoodi et al., 2012b). High stiffness to weight ratio, ease and speed of handling, as well as having favorable architectural appearance cause that, these types of structures are widely used to cover large spans without any intermediate support.

To achieve the same support conditions in both input-output and output-only modal tests, the structure was tested in free-free condition. For this goal, a double-layer grid with ball joint system was constructed in the laboratory and modal damping ratios corresponding to the first few modes of the structure (12 modes with a natural frequency below 100 Hz) were determined from input-output and output-only modal identification techniques. The methods employed in the input-output technique included Circle Fit (CF), Nonlinear Least Squares (NLLS), complex Singular Values Decomposition (SVD), and Rational Fraction Polynomials (RFP) while for output-only technique, they consisted of Enhanced Frequency-Domain Decomposition (EFDD), Curve Fitting Frequency-Domain Decomposition (CFDD), and three different methods of Data Driven Stochastic Subspace Identification (DD-SSI). Damping ratio values acquired via different output-only methods were compared with the corresponding values identified from the input-output methods.

DOUBLE-LAYER GRID

A double-layer grid with the ball joint system and a two-way on two-way configuration were constructed in the laboratory. The plan dimension of this double-layer grid was 424.2×565.6 cm and its height (distance between two layers) was 100.0 cm. As displayed in Figure 1, this grid has three 141.4 cm spans in an extension contained in the bottom layer and four 141.4 spans perpendicular to it, and generally, it consists of 96 steel pipes (with an external diameter of 7.64 cm and thickness of 0.35 cm) and 32 balls, which is similar to each other. Since the goal of this experiment has been comparing the damping under similar conditions, so the support condition must be the same during input-output and output-only testing. The grid was tested in the free-free condition whereby the structure was suspended with the help of four springs on four corner balls on the top layer of grid which had the minimum average modal displacement. More information about this grid is given in reference (Mostafavian et al., 2012).

DATA ACQUISITION

The equipment used for performing the modal tests consisted of a 4-channel spectrum analyzer (B&K PULSE 3560 C), one AP Tech impact hammer, and three DJB (A/120/V) accelerometers.

Input-Output Modal Testing

Frequency response functions of this double-layer grid were measured at the frequency range of 0-100 Hz by the impact test. Three accelerometers were mounted on the corner ball in the bottom layer of the grid in two horizontal and one vertical direction, with the impact load applied to the structure on the same ball as well as on the other balls in different directions. The impact and acceleration signals were recorded by the analyzer device within 16 seconds, with the frequency response functions obtained with a resolution of 0.0625 Hz. The appropriate degrees of freedom for applying impact and measuring the acceleration of structure were determined through modal test planning where all considered vibration modes of the structure became excited and participated to the response. To excite the grid, an impact hammer, designed for modal testing with a rubber head with a force sensor on it, was used. The impact of the hammer should have had sufficient intensity and frequency content. The intensity of the applied force was up to 480 N and force spectrum was almost straightened up until 400 Hz, which was far higher than the desired frequency ranges of 0-100 Hz. Overall, 45 Frequency Response Functions (FRF) were measured. Two of them along with their coherence functions are depicted in Figures 2 and 3. As can be seen in these figures, the coherence functions are very close to unity at the location of natural frequencies; peaks of the FRF plots.

In order to check linearity of the structure, the FRF of the two intermediate and high excitation amplitudes (maximum impact intensity of 150 N and 480 N, respectively) were measured and compared with each other. As shown in Figure 4, the results of the two excitation amplitudes are approximately identical, suggesting that in this intensity range, the behavior of structure can be assumed linear.

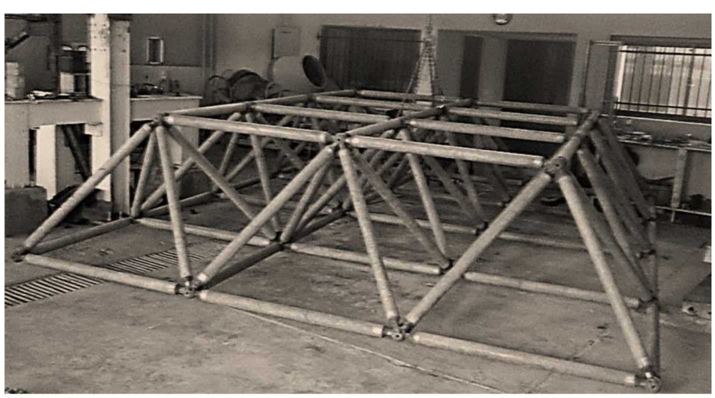

(a)

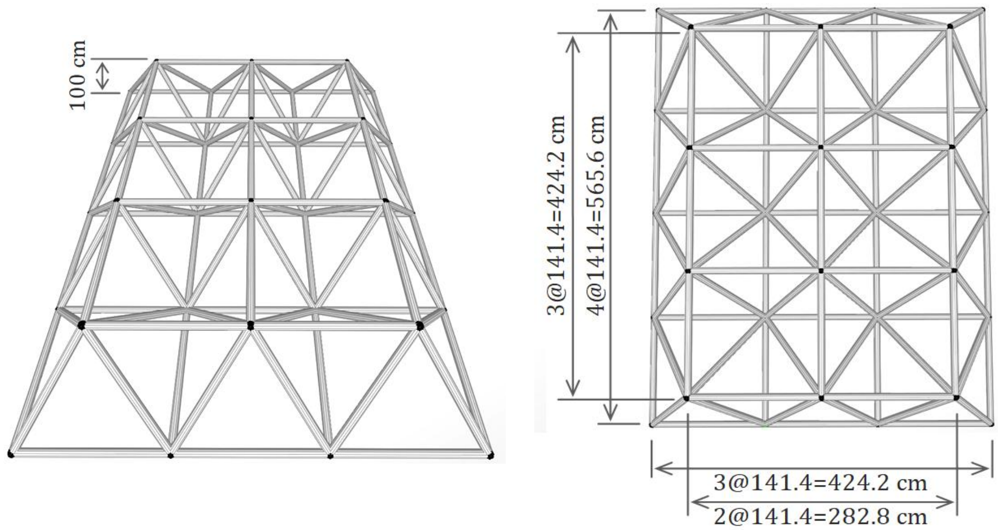

(b) **(b)**

Fig. 1. a) General view; b) plan, and; c) side view of the double-layer grid

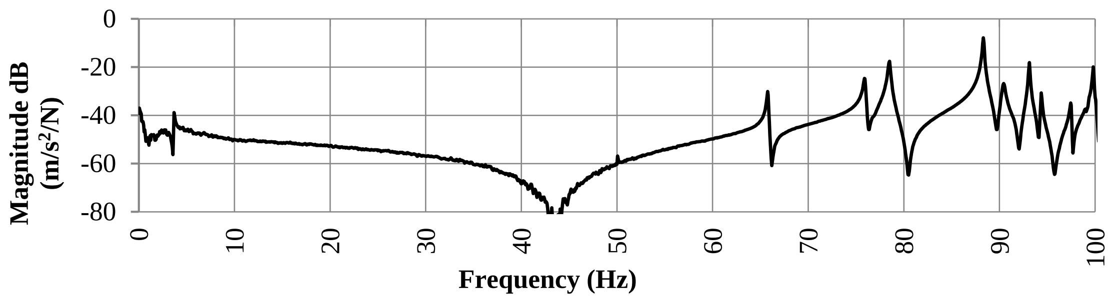

(a)

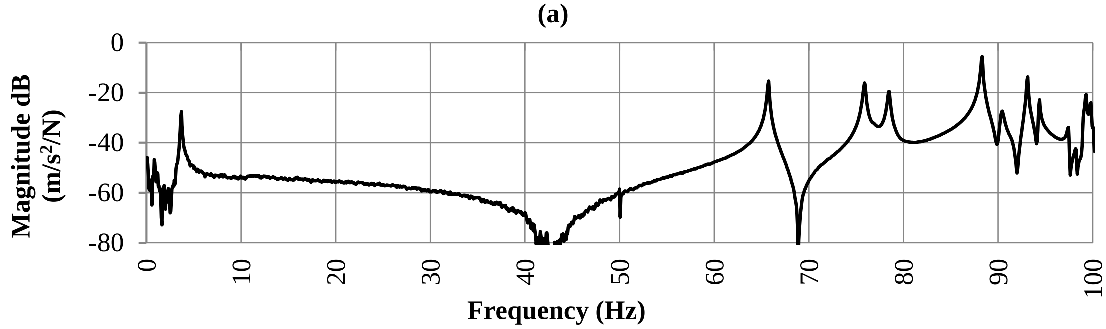

(b)

Fig. 2. a) A point FRF (impact and response are at the same degrees of freedom); b) related coherence function

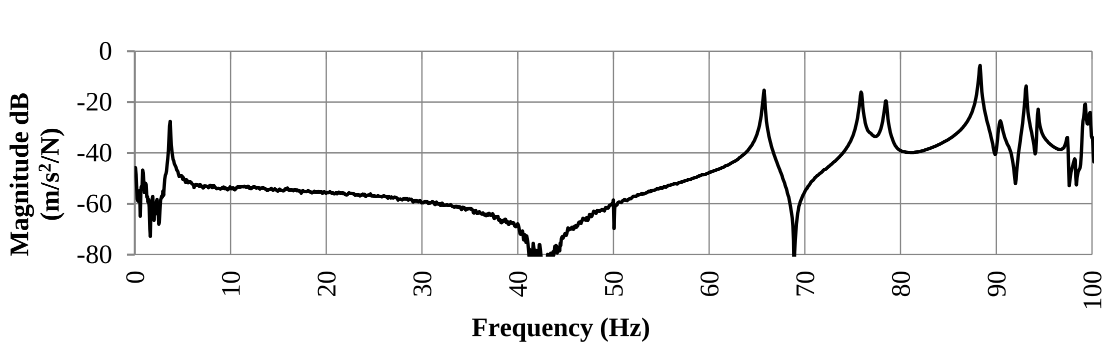

(a)

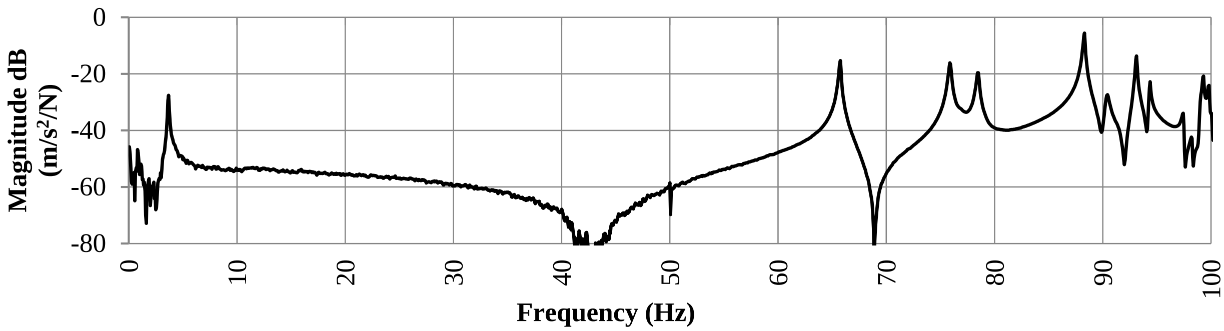

(b)

Fig. 3. a) A transfer FRF (impact and response are at different degrees of freedom); b) relevant coherence function

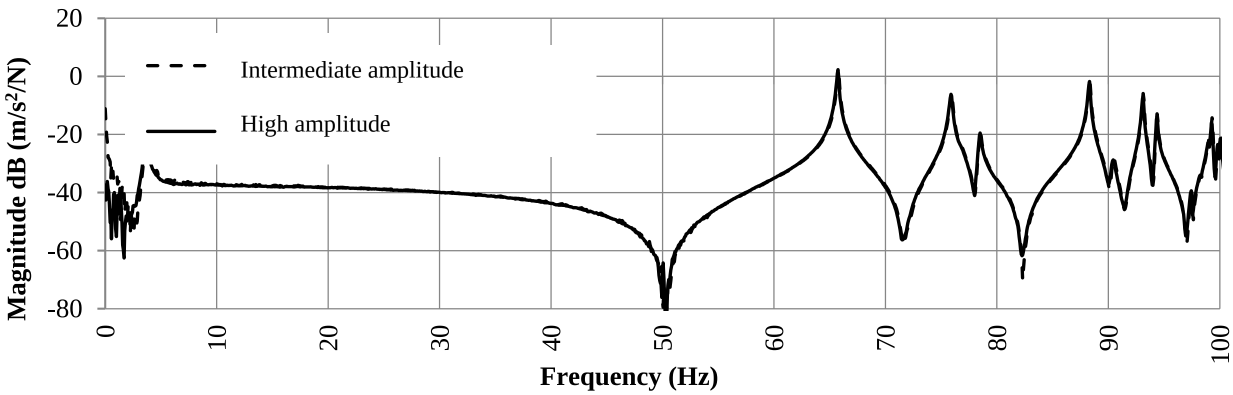

(a)

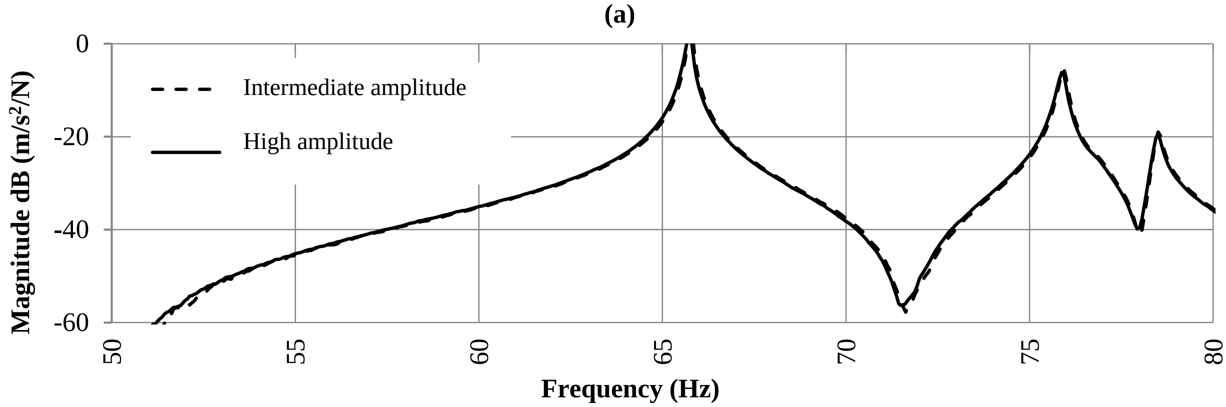

(b)

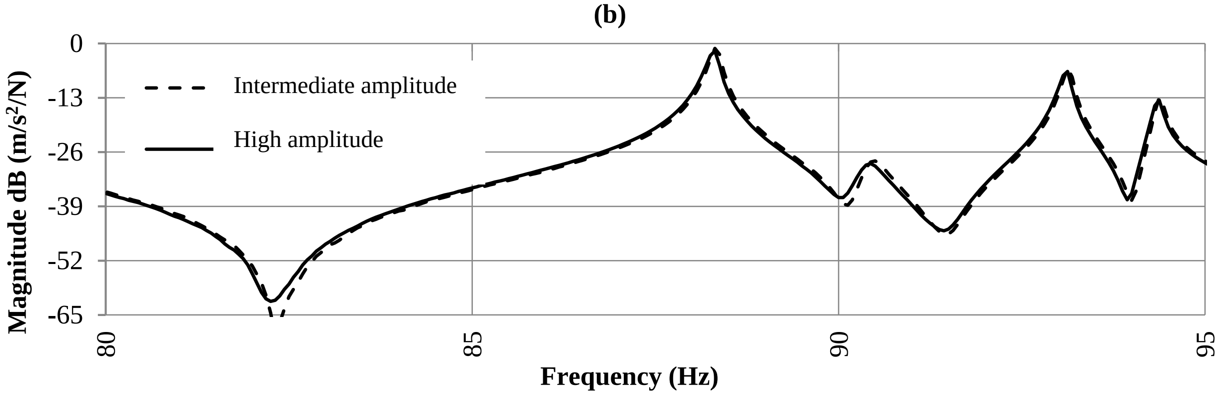

(c)

Fig. 4. a) Linearity control of the FRF by varying the amplitude of impact force; b) magnification within the range of 50-80 Hz; c) magnification within the range of 80-95 Hz

It is necessary to ensure that the structure's dynamic behavior and the whole measurement set-up system are time-invariant. For the selected force input and response locations, a structure should yield identical FRF curves for every measurement with time intervals. Figure 5 reveals the FRFs measured over a two-week interval. Comparison of these FRFs reveals that there has been no significant change in the behavior of the structure or test conditions.

Reciprocity property of the measured FRF data of the grid is illustrated in Figure 6. Exchanging the locations of force and response (measurement 1 and measurement 2), the compatibility of mutual FRFs was favorable in most areas; however, only in some areas such as anti-resonance it did not match completely, which is not an unusual phenomenon. The mismatch of mutual FRFs can have a logical reason (such as the localized characteristics of excitation and response measurement points) (He and Fu, 2001).

Output-Only Modal Testing

In order to conduct the output-only modal test, the data obtained from three accelerometers installed on the abovementioned ball of the grid in horizontal and vertical directions were used simultaneously. This ball had the maximum average modal acceleration for the desired modes of the grid. Since identification of the mode shapes of this grid was not intended, measuring one ball's acceleration was enough. The response measurement duration was chosen 840 seconds based on Brincker and Ventura's (2015) suggested relation and data acquired from the initial experiment. The structure was excited by successive tapping on the grid during response measuring time. The tapping was applied accidently to the structure in different balls and directions. The response sampling time was 0.00195 second. The sampling frequency was 512 Hz, resulting in a Nyquist frequency of 256 Hz, which was far higher than the largest natural frequency of interest, i.e. 100 Hz.

Figure 7 exhibits the Power Spectral Density (PSD) and Cross Spectral Density (CSD) functions of the response (Felber, 1994) measured across horizontal x, horizontal y and vertical z directions. As can be seen, there is an almost good agreement between the PSD and CSD plots especially in the location of peaks.

MODAL ANALYSIS

Using the measured data in two input-output and output-only modal tests, the natural frequencies and modal damping ratios from different methods were estimated.

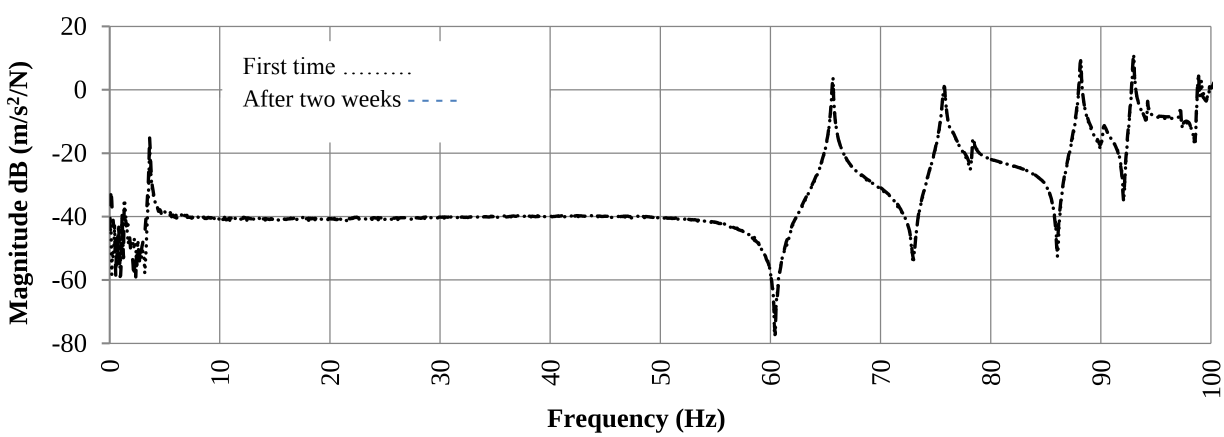

Fig. 5. Repeatability check of the measured FRF data in a two-week interval

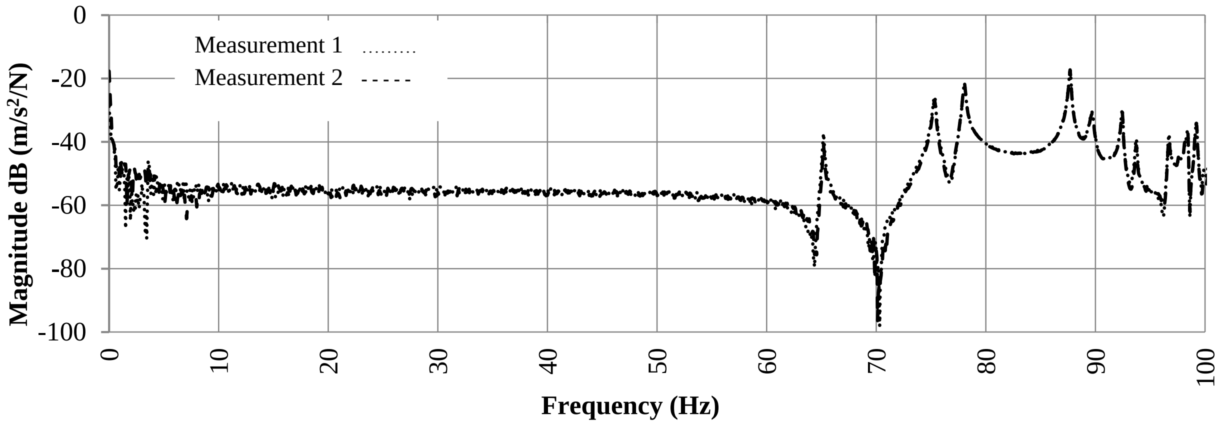

Fig. 6. Reciprocity check of the measured FRF data

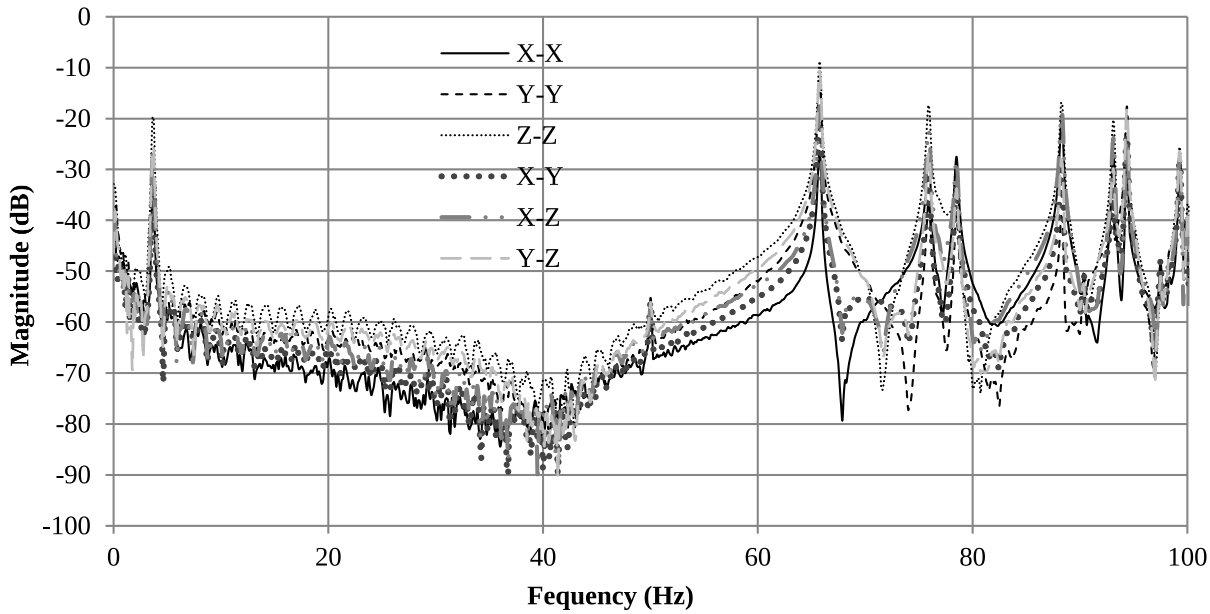

Fig. 7. PSD and CSD functions based on measured accelerations

Input-Output Modal Analysis

The natural frequencies of the grid on the FRF plot appeared in the form of local maxima, which are, indeed the resonances. FRF value at the resonance points is essentially controlled by modal damping. Therefore, by studying the FRF near the resonance points, modal damping ratios of the grid can be obtained through different methods of modal analysis.

In this paper, derivation of modal parameters from FRF data was performed through frequency-domain methods. To gain a basic general understanding of vibrational modes of the grid, initial analysis of three FRFs of the grid was done separately via circle fit method, which lies in single degree of freedom (SDoF) category. Then, using four methods of multi degrees of freedom (MDoF), 45 measured FRFs were evaluated simultaneously to extract the modal damping ratios of desired modes of the grid. There are numerous software packs for input-output modal analysis; in this study, the MODENT suite of the ICATS program was used. The input-output modal analysis methods used in the present study are briefly explained further.

Circle fit method (Ewins, 2000): The circle fit method is the most commonly used SDoF modal analysis method. It is based on the circularity of the Nyquist plot of an SDoF FRF. Drawing Nyquist plot, in which the imaginary values of the frequency response function are plotted against its real values, creates a semi-circular plot. If the suitable damping model was chosen, it becomes completely circular. In addition, Nyquist plot of MDoF FRF includes arc regions close to the circle near the natural frequencies. This feature constitutes the basis of the circle fit method.

Complex singular value decomposition method (Ewins, 2000): This method is based on a complex singular value decomposition of a system matrix expressed in terms of measured FRF properties followed by a complex eigen solution which extracts the required modal properties. The advantage of this method lies in its ability to detect very close modes.

Rational fraction polynomials method (He and Fu, 2001): This method is an MDoF modal analysis method based on measured FRF data. The idea of the rational fraction polynomial method is to express an FRF in terms of rational fraction polynomials, where through numerical manipulations, the coefficients of these polynomials can be identified. The links between these coefficients and the modal parameters of the FRF can also be established, resulting in identification of these parameters. The modal parameters are found N times (N equals to the number of measured FRFs) and averaged to yield a single consistent set.

Non-linear least squares method (He and Fu, 2001): This method is based on minimizing the difference between the measured data and a theoretical model containing a given number of modes using a non-linear least-squares approach. Here in this paper, two types of NLLS have been used namely NLLS1 and NLLS2. NLLS1 processes one FRF at a time while NLLS2 can deal with all FRFs simultaneously. Both methods require both the number of modes in a given range and initial guesses for the modal parameters of each mode. The success of the NLLS methods depends significantly on the initial guesses for the modal parameters.

Output-Only Modal Analysis

In order to extract the modal parameters via output-only method, time-domain methods of DD-SSI and the frequency-domain methods of EFDD and CFDD were employed. Three different versions of DD-SSI method known as Principal Component (PC), Unweighted Principal Component (UPC), and Canonical Variate Analysis (CVA) have been used in this paper; the difference between these versions has been explained in reference (Van Overschee and De Moor, 2012). ARTeMIS modal 4.0 software (SVS, 2015) was utilized to obtain the natural frequencies and damping ratios. Output-only modal analysis methods used in the present study are briefly explained as follows.

Stochastic subspace identification method (Zhang et al., 2012; Brincker and Andersen, 2006): The SSI method is one of the most widely used time-domain methods for output-only modal analysis. In this method, the space-state model in the discrete form is used to compute the modal parameters. Indeed, the dynamic equilibrium equation of the system, which is a second-order equation, turns into two first-order equations, called state equations and observation equations. The coefficients in these equations are called system matrices. After identifying the state space model, the modal parameters are extracted from the system matrices. To estimate the modal parameters, the state space model poles are identified and plotted in the stability diagram. The stabilization diagram is a graphical tool for estimating the optimized model parameter, which helps to distinguish the unstable and noisy poles generated by the calculation process. This, in turn, leads to the detection of the stable physical poles of the system.

Enhanced frequency-domain decomposition method (Brincker et al., 2001; Gade et al., 2005): This method adds a modal estimation layer compared to the FDD method. Modal estimation in this method involves two steps. The first step is to perform the FDD peak picking, and the second is to utilize the FDD identified mode shapes for identifying the SDoF spectral Bell function. An SDoF correlation function is obtained by transferring the SDoF spectral Bell to time domain. Then, via these correlation functions and simple regression analysis, the natural frequencies and damping ratios are obtained.

Curve-fit frequency-domain decomposition method (Jacobsen et al., 2008): As with the previous approach, the SDoF spectral Bell is formed. Natural frequencies and damping ratios of each mode are estimated by curve fitting the SDoF spectral Bell using frequency-domain least-square estimation. Since the SDoF spectral Bell is unaffected by other modes, there is a single eigenvalue and reside to fit. The natural frequencies as well as modal damping ratios are extracted from these eigenvalues.

RESULTS

Input-Output Modal Analysis Results

The results acquired from the analysis of three FRFs of the grid by CF method are summarized in Table 1. This table shows the initial approximation of the natural frequencies and the modal damping ratios of the desired modes of the grid. From the 9th to 12th modes, the difference of natural frequencies between the adjacent modes has been about 1 Hz or less, suggesting that the modes in this area are closely spaced and they are affected by each other. This has caused the 10th to 12th modes not to be estimated by the analysis of FRF function 1. Further, the identification of some modes by the analysis of FRF functions 2 and 3 found problems. It should also be noted that the 5th and 7th modes have had little contribution to function 2, where at these frequency locations, there were no local maximum or resonance in this function. The compatibility of natural frequencies obtained from the three functions, which are related to the behavior of the grid in three different directions, is highly desirable, which is a feature of a correct modal testing. However, the modal damping ratios derived from the three functions have not been fully compatible, which is not uncommon in the experimental modal analysis using SDoF methods. The problems related to the detection of close modes and damping incompatibility are far less common in MDoF methods.

The results of input-output modal analysis via MDoF methods are summarized in Table 2. The natural frequencies estimated from different methods are in good agreement with each other, as well as with the natural frequencies estimated from SDoF method (Table 1). This is a considerable result despite the different mathematical assumptions in each of these methods. According to Table 2, except for the damping of the 10th mode, which indicates a high dispersion, there is a good congruence between the modal damping ratios estimated from different methods. Further, the damping of 7th and 11th modes obtained from RFP and NLLS1 approaches, respectively, shows an irrelevant value. The final values of modal damping ratio are presented in the last column of Table 2 by averaging the results of different methods (without considering the two mentioned damping ratios). It can be observed that the studied structural system has a low damping ratio which is reasonable for a structure in free-free supporting condition without non-structural components.

The first half of the extracted modes (other than the 5th mode) has higher values of damping than the second half, which can be related to the manner of deformation of structure in each mode (or mode shape). Since in the assembled structures with separate components, a large proportion of damping is concentrated at the joints, it can be stated that any mode shape causing more deformations in the joints reveals higher values of damping. In addition, the large proportion of damping in joints results in non-proportional damping.

Output-Only Modal Analysis Results

The natural frequencies and damping ratios for the modes of interest were extracted using the methods mentioned in previous section. When using the SSI method to identify the modal parameters, an appropriate model order must be determined. The model order is indeed the number of Hankel matrix rows in this method. The minimum model order equal to 100 was selected using the initial results of input-output testing and the equation provided by Reynders and De Roeck (2008). A sensitivity analysis should be done to determine a convenient model order, as proposed by Rainieri and Fabbrocino (2014). The initial analyses indicated that the changes in the model order did not affect the values of natural frequency considerably, so sensitivity analysis was performed based on the damping values. The damping variations with respect to model order for the first to fifth modes are plotted in Figure 8. These values have been determined by the SSI-UPC method. Considering Figure 8, it can be stated that there was no convergence of damping values of the first mode as the model order increased. As can be seen later, the identified damping of the first mode in all methods indicates a greater dispersion. As presented in this figure, except for the damping corresponding to the first mode, the order of 200 can be an acceptable and optimal for this structure.

The natural frequencies and modal damping ratios identified via various SSI methods for the order of 200 are presented in Tables 3 and 4, respectively. In these tables, Std. represents values of standard deviation (at order of 200, at most 200 values of natural frequencies and damping ratios are identified in each mode; Std. is the standard deviation of these values). According to these tables, the natural frequencies and modal damping ratios associated to the 8th to 10th modes were not identified by different methods. However, the modal parameters of the 1st to 5th modes and the 11th mode were identified. As can be observed in Table 3, the estimated natural frequencies have good congruence across the methods. According to Table 4, the largest difference between damping ratios obtained via different SSI methods corresponds to the first mode. Although SSI-CVA algorithm has identified the largest number of modes compared to the two other methods, higher Std. values imply considerable scattering in the natural frequency and modal damping ratio of the grid. From this point of view, the SSI-PC is the best method. Accordingly, fewer numbers of modes have been identified by output-only methods than input-output methods which has already been reported by other researchers such as Mbarek et al. (2018).

The natural frequencies and damping ratios identified by EFDD and CFDD methods are shown in Table 5. Since the resolution of the FRFs in the input-output modal analysis was 0.0625 Hz, spectral functions in the output-only modal analysis were also considered with the same resolution. As can be seen in Table 5, modal parameters related to the 10th and 12th modes were not identified. Further, the natural frequencies estimated via the two methods have been in good agreement with each other, such that the maximum relative deviation of the natural frequency values was 0.021%. In the case of modal damping ratio, the first mode indicates greater deviation between the two methods, while in other modes, there is a good agreement between the damping ratios identified through the two methods. Also, the estimated modal damping ratios through EFDD are mostly higher than the corresponding ratios through CFDD.

Table 1. Results of the input-output modal analysis of the grid by an SDoF method of circle fit

Mode number	FRF 1		FRF 2		FRF 3	
	Frequency (Hz)	Damping (%)	Frequency (Hz)	Damping (%)	Frequency (Hz)	Damping (%)
1	3.64	8.72	3.67	3.29	3.67	3.43
2	65.75	0.402	65.78	0.374	65.78	0.26
3	75.90	0.329	75.94	0.379	75.92	0.30
4	78.47	0.346	78.49	0.318	78.49	0.31
5	88.30	0.242	----	----	88.33	0.19
6	90.40	0.678	90.42	0.431	90.43	0.43
7	93.11	0.161	----	----	93.13	0.25
8	94.35	0.301	94.37	0.214	94.37	0.17
9	97.47	0.199	97.49	0.184	97.48	0.21
10	----	----	98.30	0.146	----	----
11	----	----	99.31	0.268	99.32	0.18
12	----	----	----	----	99.82	0.13

Table 2. Results of the input-output modal analysis of the grid via four MDoF methods

Mode number	SVD		RFP		NLLS1		NLSS2		Mean	
	Frequency (Hz)	Damping (%)	Frequency (Hz)	Damping (%)	Frequency (Hz)	Damping (%)	Frequency (Hz)	Damping (%)	Frequency (Hz)	Damping (%)
1	3.66	0.31	3.67	0.33	3.67	0.34	3.67	0.39	3.67	0.34
2	65.73	0.23	65.85	0.25	65.90	0.21	65.74	0.24	65.81	0.23
3	75.89	0.30	75.98	0.33	75.98	0.27	75.89	0.30	75.94	0.30
4	78.48	0.31	78.50	0.29	78.52	0.29	78.48	0.29	78.50	0.29
5	88.29	0.17	88.31	0.17	88.32	0.16	80.33	0.17	88.31	0.17
6	90.40	0.42	90.46	0.42	90.48	0.44	90.41	0.45	90.44	0.43
7	93.11	0.14	93.18	0.27	93.13	0.14	93.11	0.15	93.13	0.14
8	94.35	0.13	94.39	0.14	94.40	0.14	94.36	0.14	94.38	0.14
9	97.48	0.15	97.41	0.15	97.40	0.15	97.48	0.17	97.44	0.15
10	98.27	0.17	98.24	0.20	98.21	0.11	98.29	0.13	98.25	0.15
11	99.27	0.14	99.29	0.14	99.39	0.45	99.28	0.14	99.31	0.14
12	99.77	0.13	99.82	0.15	99.82	0.13	99.81	0.14	99.81	0.14

Table 3. Natural frequencies of the grid obtained by the different SSI methods as well as their Stds

Mode number	Method					
	UPC		PC		CVA	
	Freq. (Hz)	Std. (Hz)	Freq. (Hz)	Std. (Hz)	Freq. (Hz)	Std. (Hz)
1	3.67	0.00	3.68	0.00	3.68	0.00
2	65.74	0.00	65.75	0.00	65.75	0.09
3	75.90	0.01	75.89	0.00	75.90	0.02
4	78.48	0.00	78.49	0.00	78.49	0.01
5	88.28	0.00	88.29	0.02	88.29	0.00
6	-	-	-	-	90.40	0.12
7	93.08	0.01	-	-	-	-
8	-	-	-	-	-	-
9	-	-	-	-	-	-
10	-	-	-	-	-	-
11	99.28	0.02	99.29	0.01	99.29	0.01
12	-	-	-	-	99.81	0.07

Table 4. Modal damping ratios of the grid obtained via the different SSI methods as well as their Stds

Mode number	Method					
	UPC		PC		CVA	
	Damping (%)	Std. (%)	Damping (%)	Std. (%)	Damping (%)	Std. (%)
1	1.03	0.24	0.35	0.06	0.32	0.23
2	0.06	0.00	0.06	0.00	0.09	0.13
3	0.10	0.01	0.10	0.00	0.10	0.02
4	0.11	0.00	0.10	0.00	0.09	0.01
5	0.06	0.00	0.06	0.01	0.06	0.04
6	-	-	-	-	0.19	0.07
7	0.08	0.01	-	-	-	-
8	-	-	-	-	-	-
9	-	-	-	-	-	-
10	-	-	-	-	-	-
11	0.10	0.01	0.09	0.00	0.07	0.03
12	-	-	-	-	0.21	0.08

Table 5. Natural frequencies and damping ratios obtained via EFDD and CFDD methods

Mode number	EFDD		CFDD	
	Frequency (Hz)	Damping (%)	Frequency (Hz)	Damping (%)
1	3.68	1.14	3.68	5.71
2	65.76	0.09	65.76	0.08
3	75.91	0.11	75.91	0.10
4	78.50	0.10	78.49	0.09
5	88.30	0.07	88.30	0.07
6	90.35	0.06	90.35	0.06
7	93.11	0.06	93.11	0.05
8	94.37	0.04	94.37	0.04
9	97.52	0.10	97.50	0.09
10	-	-	-	-
11	99.30	0.05	99.30	0.04
12	-	-	-	-

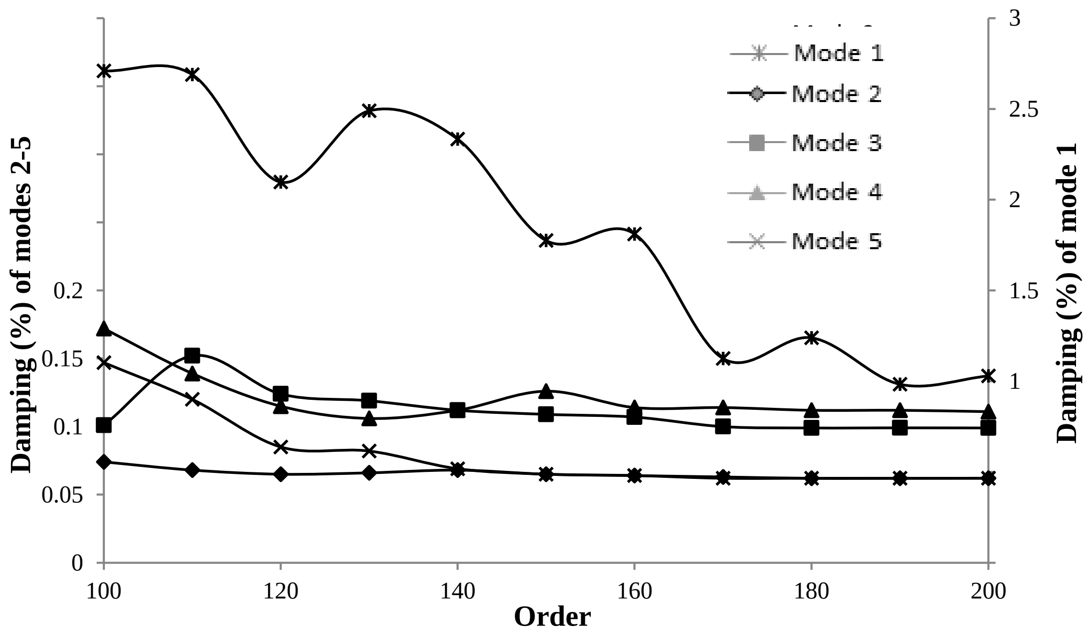

Fig. 8. Damping variations of the first to fifth modes of the grid with respect to different orders

Comparing the results of natural frequencies and damping ratios between the frequency-domain methods (EFDD and CFDD) and time-domain methods (SSI-PC, SSI-PC and SSI-CVA), it can be stated that, time-domain methods have identified fewer number of modes compared to the frequency-domain methods. The only mode both methods failed to identify was the grid's 10th mode.

COMPARISON AND DISCUSSION

Since the modal parameters obtained via input-output modal analysis have less uncertainty compared to the output-only modal analysis techniques (Magalhães et al., 2010), the mean values of Table 2 are considered as reference values with the results identified through output-only modal analysis compared with them. The relative difference of natural frequencies obtained by different methods of SSI, EFDD, and CFDD with respect to the reference values are given in Table 6. As the first five modes of the grid were identified in all methods, the comparison was made for these modes. The greatest relative difference between the natural frequencies belonged to the first mode and equaled 0.27%. In other modes, the natural frequencies estimated via input-output and output-only modal analysis techniques were very close to each other. Apart from the first mode, the natural frequencies estimated by the output-only modal analysis techniques were lower than those of the input-output modal analysis approaches.

The relative difference of damping ratios between the various methods of output-only modal analysis and the corresponding reference is presented in Table 7. As can be seen in this table, the difference values of damping ratios are significant. The values of modal damping related to the first mode identified via SSI-PC and SSI-CVA are very close to the corresponding reference magnitudes. On the other hand, the other methods show great dispersion. The modal damping ratios of the first mode obtained by SSI-UPC, FED and CFDD methods reveal a great difference with respect to the reference values. The negative signs in the table modes reflected the fact that the damping ratios estimated via different methods of output-only are less than the corresponding values, which is not consistent with the results of Avitable (2006) and Lauwagie et al. (2006). Apart from the modal damping ratio of the first mode, the average relative difference of damping has been -65% in all modes.

Table 6. Relative difference (%) of frequencies between the output-only modal analysis techniques and the reference values

Mode number	SSI-UPC	SSI-PC	SSI-CVA	EFDD	CFDD
1	0.00	0.27	0.27	0.27	0.27
2	-0.11	-0.09	-0.09	-0.08	-0.08
3	-0.05	-0.07	-0.05	-0.04	-0.04
4	-0.03	-0.01	-0.01	0.00	-0.01
5	-0.03	-0.02	-0.02	-0.01	-0.01

Table 7. Relative difference (%) of the damping ratios between output-only modal analysis methods and the corresponding values

Mode number	SSI-UPC	SSI-PC	SSI-CVA	EFDD	CFDD
1	202.94	2.94	-5.88	235.29	1579.41
2	-73.91	-73.91	-60.78	-60.78	-65.20
3	-66.67	-66.67	-66.67	-63.33	-66.67
4	-62.07	-65.52	-68.97	-65.52	-68.97
5	-65.71	-65.71	-65.71	-58.82	-58.82

Although the structure's supporting conditions in two input-output and output-only modal testing has been the same, the estimated damping ratios are different in the two techniques, which is not in accordance with Orlowitz and Brandt (2017). It is concluded that the complexity of the structure also affects the difference in damping values obtained via the two methods, which is in line with the result of Thibault et al. (2012).

CONCLUSIONS

In this paper, the modal damping ratios and also natural frequencies corresponding to the modes with frequencies less than 100 Hz (12 modes) were determined for a double-layer grid with ball joint system where the results of input-output and output-only modal analysis were compared to each other. More than half of the natural frequencies lied in a relatively small range of 90-100 Hz. The values of estimated modal damping ratios were relatively low (fraction of 1%). The results of four different methods of input-output modal analysis were in good congruence with each other, such that there was a small deviation in the estimation of modal damping ratios and natural frequencies between these methods. Five different methods were employed for output-only modal analysis with the results indicating that time-domain methods estimate fewer modes than frequency-domain methods do. The estimated natural frequencies through different output-only methods were very close together. The difference of modal damping ratios between various methods of output-only was relatively higher than the difference of natural frequencies. The dispersion of the damping estimation in the output-only modal analysis methods was not generally identified in this work.

The results of the present study indicated that the input-output modal analysis identified a greater number of modes compared to output-only modal analysis. Comparison of the results of input-output and output-only modal analysis indicated that the natural frequencies estimated through these two approaches were very close to each other. The differences in estimated damping ratios between the input-output and output-only modal analysis were greater than the differences in natural frequencies. Apart from the first mode, the damping ratios estimated via input-output modal analysis were greater than those from output-only modal analysis. Despite the uniformity of the double layer grid condition and the similarity of experimental conditions, the damping ratios obtained from two techniques of input-output and output-only modal analysis have been significantly different due to the complex behavior of the grid.

REFERENCES

Avitabile, P. (2006). "Modal space: Someone told me that operating modal analysis produces better results and that damping is much more realistic", *Experimental Techniques*, 30 (6), 25-26.

Azam, S.E., Mariani, S. and Attari, N.K.A. (2017). "Online damage detection via a synergy of proper orthogonal decomposition and recursive Bayesian filters", *Nonlinear Dynamics*, 89(2), 1489-1511.

Beskhyroun, S., Wotherspoon, L.M. and Ma, Q.T. (2013). "System identification of a 13-Story reinforced concrete building through ambient and forced vibration", *4th International Conference on Computational Methods in Structural Dynamics and Earthquake Engineering (COMPDYN)*, Kos Island, Greece.

Brincker, R., Ventura, C.E. and Andersen, P. (2001). "Damping estimation by frequency domain decomposition", *Proceedings of the 19th International Modal Analysis Conference (IMAC)*, February 5-8, The Hyatt Orlando, Kissimmee, Florida, pp. 698-703.

Brincker, R., Ventura, C. and Andersen, P. (2003). "Why output-only modal testing is a desirable tool for a wide range of practical applications", *Proceedings of IMAC-21: A Conference on Structural Dynamics*, February 3-6, The Hyatt Orlando, Kissimmee, Florida, pp. 265-272.

Brincker, R. and Andersen, P. (2006). "Understanding stochastic subspace identification", *Proceedings of the 24th (IMAC)*, The Hyatt Orlando, Kissimmee, Florida, pp. 279-311.

Brincker, R. and Kirkegaard, P.H. (2010). "Special issue on operational modal analysis", *Mechanical Systems and Signal Processing*, 5(24), 1209-1212.

Brincker, R. and Ventura, C. (2015). *Introduction to operational modal analysis*, John Wiley and Sons.

Chopra, A.K. (2001). *Dynamics of structures: Theory and applications to earthquake engineering*, Prentice Hall.

Davoodi, M.R., Navayi Neya, B., Mostafavian, S.A., Nabavian, S.R. and Jahangiry, Gh.R. (2017). "Determining minimum number of required accelerometer for output-only structural identification of frames", *7th International Operatuinal Modal Analysis Conference "IOMAC2017"*, May 10-12, Ingolstadt, Germany.

Davoodi, M.R., Mahdavi, M. and Mostafavian, S.A. (2012). "Experimental and analytical determination of dynamic properties of a steel frame with bolted flange joints", *Proceedings of International Conference on Engineering and Information Technology "ICEIT2012"*, September, Toronto, Canada, pp. 17-18.

Davoodi, M.R., Amiri, J.V., Gholampour, S. and Mostafavian, S.A. (2012). "Determination of nonlinear behavior of a ball joint system by model updating", *Journal of Constructional Steel Research*, 71, 52-62.

De Almeida Cardoso, R., Cury, A., Barbosa, F. and Gentile, C. (2019). "Unsupervised real-time SHM technique based on novelty indexes", *Structural Control and Health Monitoring*, 26(7), e2364.

Dertimanis, V.K., Chatzi, E.N., Azam, S.E. and Papadimitriou, C. (2019). "Input-state-parameter estimation of structural systems from limited output information", *Mechanical Systems and Signal Processing*, 126, 711-746.

Ewins, D.J. (2000). *Modal testing : Theory, practice, and application*, John Wiley & Sons.

Felber, A.J. (1994). "Development of a hybrid bridge evaluation system", Ph.D. Thesis, University of British Columbia.

Gade, S., Møller, N., Herlufsen, H. and Konstantin-Hansen, H. (2005). "Frequency domain techniques for operational modal analysis", *The 1st IOMAC Conference*, April 26, Copenhagen, Denmark.

Giraldo, D.F., Song, W., Dyke, S.J. and Caicedo, J.M. (2009). "Modal identification through ambient vibration: Comparative study", *Journal of Engineering Mechanics*, 135 (8), 759-770.

Gomes, J., Pereira, S., Magalhães, F., Lemos, J.V. and Cunha, A. (2018). "Input-output vs output-only modal identification of Baixo Sabor Concrete Arch Dam", T*he 9th European Workshop on Structural Health Monitoring*, July 10-13, Manchester, United Kingdom.

He, J. and Fu, Z.F. (2001). *Modal analysis*, Butterworth-Heinemann.

Jacobsen, N.J., Andersen, P. and Brincker, R. (2008). "Applications of frequency domain curve-fitting in the EFDD technique", *Proceedings IMAC XXVI Conference*, February 4, Orlando, Florida, United States.

Lauwagie, T., Van Assche, R., Van der Straeten, J. and Heylen, W. (2006). "A comparison of experimental, operational, and combined experimental-operational parameter estimation techniques", *Proceedings of the International Noise and Vibration Conference, ISMA*, September 1, Heverlee, Belgium, pp. 2997-3006.

Magalhães, F., Cunha, A., Caetano, E. and Brincker, R. (2010). "Damping estimation using free decays and ambient vibration tests", *Mechanical Systems and Signal Processing*, 24 (5), 1274-1290.

Mbarek, A., Del Rincon, A., Hammami, A., Iglesias, M., Chaari, F., Viadero, F. and Haddar, M. (2018). "Comparison of experimental and operational modal analysis on a back to back planetary gear", *Mechanism and Machine Theory*, 124, 226-247.

Mostafavian, S.A., Davoodi, M.R. and Vaseghi Amiri, J. (2012). "Ball joint behavior in a double layer grid by dynamic model updating", *Journal of Constructional Steel Research*, 76, 28-38.

Orlowitz, E. and Brandt, A. (2017). "Comparison of experimental and operational modal analysis on a laboratory ttest plate", *Measurement*, 102(May), 121-130.

Perez-Ramirez, C.A., Amezquita-Sanchez, J.P., Valtierra-Rodriguez, M., Adeli, H., Dominguez-Gonzalez, A. and Romero-Troncoso, R.J. (2019). "Recurrent neural network model with Bayesian training and mutual information for response prediction of large buildings", *Engineering Structures*, 178, 603-615.

Qarib, H. and Adeli, H. (2016). "A comparative study of signal processing methods for structural health monitoring", *Journal of Vibroengineering*, 18(4), 2186-2204.

Qarib, H. and Adeli, H. (2015). "A new adaptive algorithm for automated feature extraction in exponentially damped signals for health monitoring of smart structures", *Smart Materials and Structures*, 24(12), 125040.

Rainieri, C. and Fabbrocino, G. (2014) "Influence of model order and number of block rows on accuracy and precision of modal parameter estimates in stochastic subspace identification", *International Journal of Lifecycle Performance Engineering* 10, 1(4), 317-334.

Reynders, E. and De Roeck, G. (2008). "Reference-based combined deterministic–stochastic subspace identification for experimental and operational modal analysis", *Mechanical Systems and Signal Processing*, 22(3), 617-637.

Rezaifar, O. and Doost Mohammadi, M.R. (2016). "Damage detection of axially loaded beam: A frequency-based method", *Civil Engineering Infrastructures Journal*, 49(1), 165-172.

Sestieri, A. and D'ambrogio, W. (2003). "Frequency response function versus output-only modal testing identification", *Proceedings of 21st IMAC*, 3-6 February, Kissimmee, Florida, pp. 41-46.

Sony, S., Laventure, S. and Sadhu, A. (2019). "A literature review of next- generation smart sensing technology in structural health monitoring", *Structural Control and Health Monitoring*, 26(3), e2321.

Srikantha Phani, A. and Woodhouse, J. (2007). "Viscous damping identification in linear vibration", *Journal of Sound and Vibration*, 303 (3-5), 475-500.

Structural Vibration Solutions (SVS). (2015). *ARTeMIS Modal 4*, Denmark.

Thibault, L., Marinone, T. Avitabile, P. and van Karsenvan, C. (2012). "Comparison of modal parameters estimated from opproaches", In: *Topics in Modal Analysis I*, Volume 5, 77-88, Springer.

Van Overschee, P. and De Moor, B.L. (2012). *Subspace identification for linear systems: Theory-implementation-applications*, Springer Science and Business Media.

Yasi, B. and Mohammadizadeh, M.R. (2018). "Identification of structural defects using computer algorithms", *Civil Engineering Infrastructures Journal*, 51(1), 55-86.

Zhang, G., Tang, B. and Tang, G. (2012). "An improved stochastic subspace identification for operational modal analysis", *Measurement*, 45(5), 1246-1256.